Equivalent Network Representation of Boundary Conditions Involving Generalized Trial Quantities—Application to Lossy Transmission Lines with Finite Metallization Thickness

Farid Bouzidi, Hervé Aubert, *Member, IEEE*, Damienne Bajon, and Henri Baudrand, *Senior Member, IEEE*

***Abstract*— The derivation of integral equations for solving boundary conditions by mere application of analog Kirchhoff's and Ohm's laws is used. Generalized trial quantities are introduced as virtual adjustable sources in the equivalent network representation of boundary conditions. The lossy conductor domain of a planar transmission line is represented by a particular two-port. Thus, metallic losses can be evaluated for any metallization thickness without restricting the conductor modeling to a simple surface impedance approximation. In this paper, this two-port model is discussed and numerical results relative to a lossy coplanar waveguide (CPW) are presented. These results are in very good agreement with those obtained from the mode-matching technique and with other experimental data available in the literature. The size of matrices involved in the calculation of losses is twice as large as that in the lossless case. Moreover, the authors' formulation can be easily applied to superconducting planar transmission lines.**

I. Introduction

CONDUCTOR losses are a significant parameter for the design of monolithic microwave integrated circuits (MMIC's) due to the miniaturized dimensions and the rise of frequency; therefore, it plays an important role in the conception of highly accurate modeling tools. Recently, lossy planar transmission lines have been analyzed by a few methods which include the mode-matching technique [1]–[5], spectral-domain analysis (SDA) [6]–[12], and phenomenological equivalent method [13]. The mode-matching technique is the more direct full-wave approach for the modeling of metallic losses. It allows one to analyze lossy transmission lines with finite-metallization thickness. However, the accuracy of this approach is attributed to great numerical efforts due to determination of metal modes [1], [4]. SDA does not use generalized trial quantities and, consequently, differs from the proposed formulation [16]. As matter of fact, the calculation of conductor losses by SDA is restricted to the case of a thin [6], [7] or a thick [8]–[12] metal layer. In the first case, the trial quantity is the current density on the lossy conductor, while in the second case, it consists within a tangential electric field in the apertures of the discontinuity plane. This modeling is based either on the impedance surface approximation [7], [9]–[12] or on the perturbational method [6], [8]. Note the difficulty to determine the power lost in the conductors [14], [15] in the case of thin conductors.

For the modeling of lossy planar transmission lines, the authors have introduced [16] a particular two-port model in the equivalent network representation of boundary conditions—this two-port delivers one from any limitation in the metallization thickness and frequency range. In this paper, the impedance matrix of this two-port is given. It is shown that the equivalent network including the two-port and generalized trial quantities are more powerful than the usual surface impedance approximation. The choice of trial functions for the expansion of generalized trial quantities is also presented. In order to demonstrate the effectiveness of the proposed formulation, numerical results relative to lossy coplanar waveguides (CPW's) are given.

Manuscript received April 9, 1995; revised February 28, 1997.

F. Bouzidi and D. Bajon are with the Electronics Department, Aeronautic and Space National School, ENSAE "SupAero," 31055 Toulouse, France.

H. Aubert and H. Baudrand are with Laboratoire de Microondes, ENSEEIHT, 31071 Toulouse, France.

Publisher Item Identifier S 0018-9480(97)03908-2.

II. Formulation

In this paper, an $e^{j\omega t}$ time dependence is assumed for every field component, but is suppressed throughout. ω designates the angular frequency.

A. The Two-Port Model for a Lossy Conducting Layer

Consider a layer of lossy conductor V bounded by two regular surfaces S_1 and S_2 [Fig. 1(a)], and characterized by its electrical conductivity σ, permittivity ε, and permeability μ. From the assumptions that: 1) the local radius of surfaces curvature is larger compared to the thickness t of the layer and 2) the conductivity σ is greater than $\omega\varepsilon$, one can formulate the TEM-approximation for the electromagnetic field inside the lossy conductor [17]. Thus, the relationship between tangential electric fields and current densities infinitely closed to S_1 and

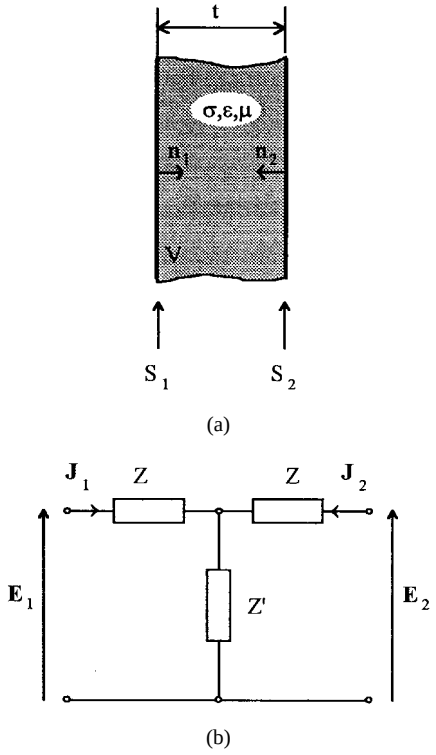

Fig. 1. (a) Layer of lossy conductor and (b) its two-port representation.

S_2 is given by the following expression:

$$\begin{bmatrix} E_1 \\ E_2 \end{bmatrix} = \begin{bmatrix} Z_{11} & Z_{12} \\ Z_{21} & Z_{22} \end{bmatrix} \cdot \begin{bmatrix} J_1 \\ J_2 \end{bmatrix} \tag{1}$$

where impedance matrix elements are

$$Z_{11} = Z_{22} = Z_\sigma \coth \gamma_\sigma t, \qquad Z_{12} = Z_{21} = \frac{Z_\sigma}{\mathrm{sh}\gamma_\sigma t} \tag{2}$$

with $Z_\sigma = \frac{1+j}{\sigma\delta}$ and $\gamma_\sigma = \frac{1+j}{\delta} \cdot \delta$ and t designate, respectively, the skin depth and layer thickness. The current density $J_i (i = 1, 2)$ has been introduced ([16, Sect. A]) and defined by

$$J_i = H_i \times n_i \tag{3}$$

where $n_i (i = 1, 2)$ designates the positive normal at points on S_i directed into V [Fig. 1(a)]. Equation (1) suggests representing the layer with a two-port. From (2), the T-network representation of this two-port brings out two impedances Z and Z' [see Fig. 1(b)], which are given by

$$Z = Z_\sigma \left[\coth \gamma_\sigma t - \frac{1}{\mathrm{sh}\gamma_\sigma t} \right], \qquad Z' = \frac{Z_\sigma}{\mathrm{sh}\gamma_\sigma t}. \tag{4}$$

For a *thin* layer (i.e., the thickness t is smaller than skin depth δ) the impedance Z is negligible in comparison with Z'. In fact, when $t \ll \delta$, (4) implies $Z \approx 0$ and $Z' \approx \frac{1}{\sigma t}$. Consequently, the network representation of this layer [Fig. 2(a)] is reduced to a single surface impedance $Z_{s_{\mathrm{thin}}}$, which is given by

$$Z_{s_{\mathrm{thin}}} \equiv \frac{1}{\sigma t} \tag{5}$$

which is the model usually applied to thin conducting strips [19], [20]. The surface impedance definition (5) does not depend on the frequency (some authors have used another definition, i.e., $Z_{s_{\mathrm{thin}}} \equiv \frac{1}{\sigma\delta}$, in order to take into account frequency dependence [7]).

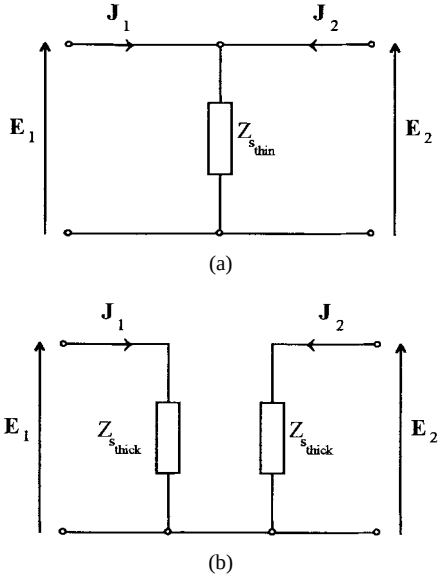

Fig. 2. Two-port models for a (a) thin and (b) thick conducting layer.

For a *thick* layer (i.e., the thickness t is greater than a few skin depths δ) the shunt impedance Z' is negligible in comparison with Z. Consequently, when $t \gg \delta$, (2) implies $Z_{12} = Z_{21} \approx 0$, and (4) gives $Z \approx Z_\sigma \coth \gamma_\sigma t$ and $Z' \approx 0$. The network representation of such a layer is then reduced to Fig. 2(b) with

$$Z_{s_{\mathrm{thick}}} \equiv Z_\sigma \coth \gamma_\sigma t. \tag{6}$$

The usual surface impedance model for transmission lines with thick conducting strips introduces the same relationship [18], [19].

B. Derivation of Integral Equations

Consider in Fig. 3(a) a suspended CPW shielding with finite-metallization thickness and isotropic lossless dielectric inside a rectangular waveguide with perfect electric conducting walls. Due to the symmetry at the plane $x = \frac{a}{2}$, only one half of the structure is considered. An $e^{-j\beta z} z$-dependence is assumed for every field component and β designates the unknown complex propagation constant.

Let D be the surface on which boundary and continuity conditions are required. The equivalent network representation of boundary conditions is established in [16], and is reported in Fig. 4. This network introduces generalized trial quantities defined on the aperture subdomain S_a in D. Note that a dual equivalent network [Fig. 5(a)] could be built with generalized trial quantities defined on the lossy conductor subdomain S_b in D (in Fig. 5(b) and 5(c), the network representations of boundary conditions on the two subdomains S_a and S_b are given, respectively). In Fig. 4, impedance operators $\hat{Z}$ and $\hat{Z}'$ have replaced the scalar impedances Z and Z' introduced in the preceding paragraph. In fact, these operators are related to

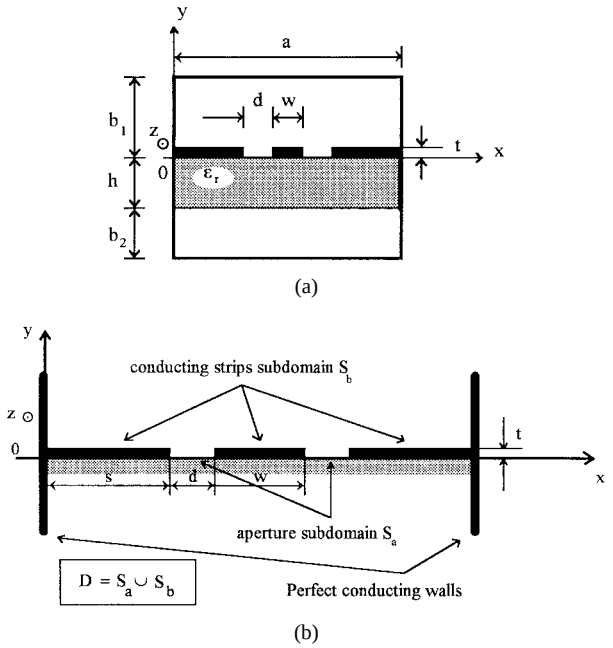

Fig. 3. (a) Cross-sectional view of the CPW under consideration. (b) The entire domain D where boundary and continuity conditions are required.

the scalar impedances by the following relationships:

$$\hat{Z} = Z 1_D \quad \text{and} \quad \hat{Z}' = Z' 1_D \tag{7}$$

where 1_D designates the unit operator; by definition, for any quantity F defined in D, one has $1_D F = \hat{F}$.

The relationship between the trial quantities and their dual has been derived [16, eq. (10)] from analog Kirchhoff's and Ohm's laws applied to the equivalent network representation of Fig. 4 as follows:

$$\begin{bmatrix} J \\ E \end{bmatrix} = \begin{bmatrix} \hat{H}_{11} & \hat{H}_{12} \\ \hat{H}_{21} & \hat{H}_{22} \end{bmatrix} \cdot \begin{bmatrix} E_{\text{tri}} \\ J_{\text{tri}} \end{bmatrix} \tag{8a}$$

with

$$\begin{aligned} \hat{H}_{11} &= (\hat{Z}_1 + \hat{Z}_2 + 2\hat{Z})\hat{D}^{-1} \\ \hat{H}_{12} &= -\hat{H}_{21} = \hat{Z}(\hat{Z}_1 - \hat{Z}_2)\hat{D}^{-1} \\ \hat{H}_{22} &= 2\hat{Z}\left(\hat{Z}_1\hat{Z}_2 + (\hat{Z}_1 + \hat{Z}_2)\left(\hat{Z}' + \frac{1}{2}\hat{Z}\right)\right)\hat{D}^{-1} \end{aligned} \tag{8b}$$

where $\hat{D} = (\hat{Z}_1 + \hat{Z})(\hat{Z}_2 + \hat{Z}) + (\hat{Z}_1 + \hat{Z}_2 + 2\hat{Z})\hat{Z}'$. Moreover, following the fundamental principle given in [16, Sect. B-2], E and J have to be determined in order to ensure that the trial quantities E_{tri} and J_{tri} do not supply power into domain D. Thus

$$\begin{bmatrix} J \\ E \end{bmatrix} = \begin{bmatrix} 0 \\ 0 \end{bmatrix} \text{ on } S_a. \tag{9}$$

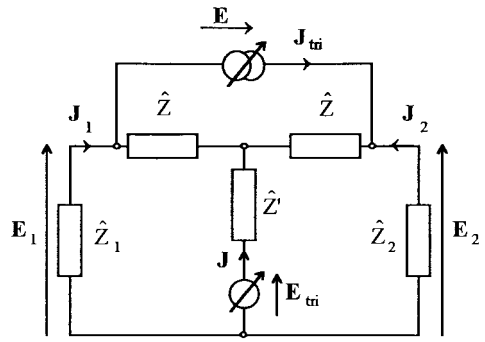

Fig. 4. Equivalent network representation with trial quantities defined on the aperture subdomain S_a.

Consequently, one can deduce from (8) and (9) the formal set of integral equations

$$\begin{bmatrix} \hat{H}_{11} & \hat{H}_{12} \\ \hat{H}_{21} & \hat{H}_{22} \end{bmatrix} \cdot \begin{bmatrix} E_{\text{tri}} \\ J_{\text{tri}} \end{bmatrix} = \begin{bmatrix} 0 \\ 0 \end{bmatrix} \text{ on } S_a. \tag{10}$$

Well-known results in three special cases [21] will now be retrieved.

Lossless Case: When the conductors are assumed to be perfect (i.e., for infinite conductivity σ), the impedances Z and Z', given in (4), are zero. Therefore, (10) becomes

$$\begin{bmatrix} (\hat{Y}_1 + \hat{Y}_2) & 0 \\ 0 & 0 \end{bmatrix} \cdot \begin{bmatrix} E_{\text{tri}} \\ J_{\text{tri}} \end{bmatrix} = \begin{bmatrix} 0 \\ 0 \end{bmatrix} \text{ on } S_a \tag{11}$$

where $\hat{Y}_i = \hat{Z}_i^{-1} (i = 1, 2)$ designates the admittance operator. Then the integral equation to solve in that case is given by

$$(\hat{Y}_1 + \hat{Y}_2) E_{\text{tri}} = 0 \text{ on } S_a. \tag{12}$$

This equation has already been derived from the direct study of a lossless finline [16]. Moreover, note that the set of integral equations (10) involved in the lossy case is only twice as large as (12), which is associated with the lossless case.

Thin Conducting Strips Case: In this case, from (5) and (10) one deduces

$$\begin{bmatrix} \left((\hat{Y}_1 + \hat{Y}_2)^{-1} + \hat{Z}_{s_{\text{thin}}}\right)^{-1} & 0 \\ 0 & 0 \end{bmatrix} \cdot \begin{bmatrix} E_{\text{tri}} \\ J_{\text{tri}} \end{bmatrix} = \begin{bmatrix} 0 \\ 0 \end{bmatrix} \text{ on } S_a \tag{13}$$

where $\hat{Y}_i = \hat{Z}_i^{-1} (i = 1, 2)$. Therefore, the integral equation to solve in the case of a CPW with thin conducting strips is

$$\left((\hat{Y}_1 + \hat{Y}_2)^{-1} + \hat{Z}_{s_{\text{thin}}}\right)^{-1} E_{\text{tri}} = 0 \text{ on } S_a. \tag{14}$$

Thick Conducting Strips Case: Equations (6) and (10) imply $\hat{D} = (\hat{Z}_1 + \hat{Z}_{s_{\text{thick}}})(\hat{Z}_2 + \hat{Z}_{s_{\text{thick}}})$. Equation (15), shown at the bottom of the page, designates the set of integral equations to solve in the case of a CPW with thick conducting strips.

$$\hat{D}^{-1} \begin{bmatrix} (\hat{Z}_1 + \hat{Z}_2 + 2\hat{Z}_{s_{\text{thick}}}) & \hat{Z}_{s_{\text{thick}}}(\hat{Z}_1 - \hat{Z}_2) \\ \hat{Z}_{s_{\text{thick}}}(\hat{Z}_2 - \hat{Z}_1) & 2\hat{Z}_{s_{\text{thick}}}(\hat{Z}_1\hat{Z}_2 + (\hat{Z}_1 + \hat{Z}_2)\hat{Z}_{s_{\text{thick}}}/2) \end{bmatrix} \cdot \begin{bmatrix} E_{\text{tri}} \\ J_{\text{tri}} \end{bmatrix} = \begin{bmatrix} 0 \\ 0 \end{bmatrix} \quad \text{on } S_a \tag{15}$$

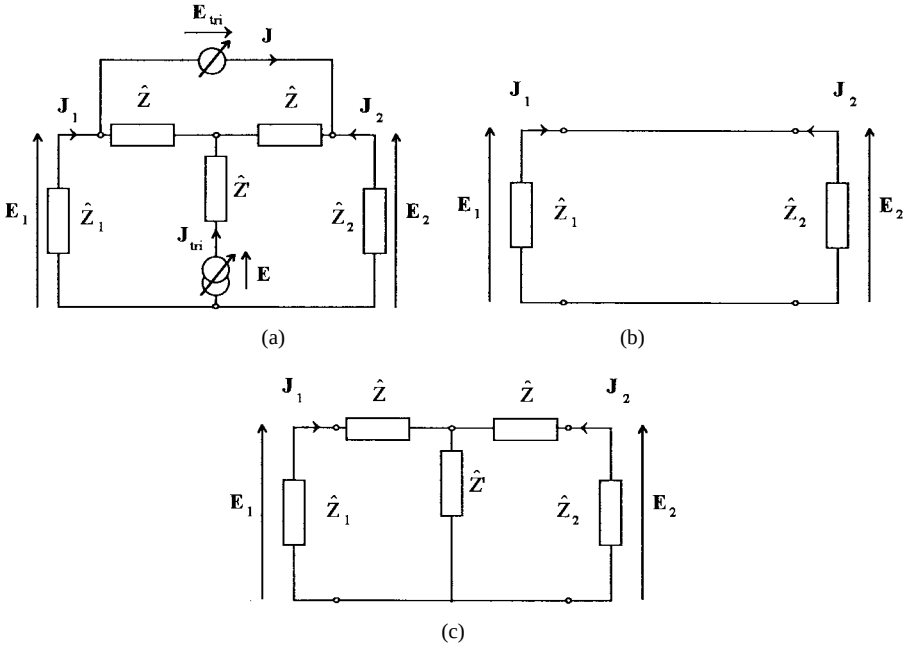

Fig. 5. Equivalent network representations with trial quantities defined on the lossy conductor subdomain S_b in (a) the entire domain D, (b) in the subdomain S_a, and (c) in the subdomain S_b.

C. The Entire Domain Trial Functions

For the resolution of integral equations (10), E_{tri} and J_{tri} are expanded on two sets of trial functions g_p and $h_{p'}$, respectively, which are defined in the entire aperture subdomain S_a

$$E_{\text{tri}} = \sum_{p=1}^{P} e_p g_p \quad \text{and} \quad J_{\text{tri}} = \sum_{p'=1}^{P'} j_{p'} h_{p'} \tag{16a}$$

with

$$g_{2k-1} = \begin{bmatrix} \Phi_x^{(k)}(x) \\ 0 \end{bmatrix}, \qquad g_{2k} = \begin{bmatrix} 0 \\ \Phi_z^{(k)}(x) \end{bmatrix}$$
$$h_{2k'-1} = \begin{bmatrix} \Psi_x^{(k')}(x) \\ 0 \end{bmatrix}, \quad \text{and} \qquad h_{2k'} = \begin{bmatrix} 0 \\ \Psi_z^{(k')}(x) \end{bmatrix}$$
$$\text{for } k, k' = 1, 2, \cdots. \tag{16b}$$

e_p and $j_{p'}$ designate unknown coefficients. Any kind of trial functions may be used as long as they are nonzero only on the aperture S_a. However, the accuracy of the numerical results depends greatly on the choice of these functions. Cosine trial functions are used in this paper. This choice seems to avoid the occurrence of spurious solutions for the propagation constant β [22]. Thus, for $x \in [(a-w)/2-d,\ (a-w)/2]$ one chooses the following trial functions [see Fig. 3(b)]:

$$\begin{cases} \Phi_x^{(k)}(x) = \cos((k-1)\pi(x-s)/d) \\ \Phi_z^{(k)}(x) = \sin(k\pi(x-s)/d) \end{cases}$$

and

$$\begin{cases} \Psi_x^{(k')}(x) = \sin(k'\pi(x-s)/d) \\ \Psi_z^{(k')}(x) = \cos((k'-1)\pi(x-s)/d) \end{cases} \tag{17}$$

with $s = (a-w)/2-d$, and for $x \in]0,\ (a-w)/2-d[\cup](a-w)/2, a/2[$, one lets

$$\Phi_x^{(k)}(x) = \Phi_z^{(k)}(x) = \Psi_x^{(k')}(x) = \Psi_z^{(k')}(x) = 0.$$

D. Resolution of Integral Equations

The formal set of integral equations (10) is developed by applying Galerkin's method with cosine trial functions (16), (17). One deduces the following $(P+Q)(P+Q)$ matrix form and for a nontrivial solution, one has to ensure

$$\det \begin{bmatrix} \vdots & \vdots \\ \cdots \langle g_p, \hat{H}_{11} g_q \rangle & \cdots \langle g_p, \hat{H}_{12} h_{q'+P} \rangle \cdots \\ \vdots & \vdots \\ \cdots \langle h_{p'+P}, \hat{H}_{21} g_q \rangle & \cdots \langle h_{p'+P}, \hat{H}_{22} h_{q'+P} \rangle \cdots \\ \vdots & \vdots \end{bmatrix} = 0. \tag{18}$$

Consequently, the complex propagation constant β can be deduced. At this stage, a new determinantal equation which minimizes computational efforts is derived from (18). In effect, the unknown complex wavenumber β can be determined by applying a perturbational method; thus, as will be shown, β can be deduced from *real* wavenumbers. Let β_0 be the wavenumber in the lossless case, i.e., for $(Z, Z') = (0, 0)$. Consider the change in the real part of the propagation constant due to a perturbation of the real part of Z and Z'. Let β be the perturbed propagation constant. Then, the perturbational formula is

$$\text{Re}(\beta - \beta_0) = \text{Re}(\delta\beta) = \beta_1 \text{Re}(\delta Z) + \beta_1' \text{Re}(\delta Z') \tag{19}$$

where

$$\beta_1 = \left(\frac{\partial \beta}{\partial \text{Re}(Z)} \right)_{(Z,Z')=(0,0)}$$

and

$$\beta_1' = \left(\frac{\partial\beta}{\partial \mathrm{Re}(Z')}\right)_{(Z,Z')=(0,0)}.$$

In (19), Re designates the real part, and the two complex impedances Z and Z' are given in (4). Thus, $\mathrm{Re}(\delta\beta)$ gives an approximation of the attenuation constant from the knowledge of two real numbers, namely β_1 and β_1'. These numbers are determined numerically. This perturbational method avoids numerical efforts which are associated with the determination of complex propagation constants. Moreover, it involves self-adjoint operators, namely $\hat{H}_{11}$, $\hat{H}_{12}$, $\hat{H}_{21}$, and $\hat{H}_{22}$ (8b), which are very easy to compute. Following (16b), the matrix elements of (19) depend on the parities of p and q. Let one write these elements, as shown in (20) at the bottom of the page, with

$$\begin{cases} H_{11m}^{(\alpha)} = \dfrac{2Z+Z_{1m}^{(\alpha)}+Z_{2m}^{(\alpha)}}{\left(Z_{1m}^{(\alpha)}+Z\right)\left(Z_{2m}^{(\alpha)}+Z\right)+\left(2Z+Z_{1m}^{(\alpha)}+Z_{2m}^{(\alpha)}\right)Z'} \\ H_{12m}^{(\alpha)} = -H_{21m}^{(\alpha)} = \dfrac{Z\left(Z_{1m}^{(\alpha)}-Z_{2m}^{(\alpha)}\right)}{\left(Z_{1m}^{(\alpha)}+Z\right)\left(Z_{2m}^{(\alpha)}+Z\right)+\left(2Z+Z_{1m}^{(\alpha)}+Z_{2m}^{(\alpha)}\right)Z'} \\ H_{22m}^{(\alpha)} = \dfrac{2Z\left(Z_{1m}^{(\alpha)}Z_{2m}^{(\alpha)}+\left(Z_{1m}^{(\alpha)}+Z_{2m}^{(\alpha)}\right)\left(Z'+\frac{1}{2}Z\right)\right)}{\left(Z_{1m}^{(\alpha)}+Z\right)\left(Z_{2m}^{(\alpha)}+Z\right)+\left(2Z+Z_{1m}^{(\alpha)}+Z_{2m}^{(\alpha)}\right)Z'} \end{cases} \tag{21}$$

where $Z_{1m}^{(\alpha)}$ and $Z_{2m}^{(\alpha)}$ designate the mth α-modal impedances ($\alpha = \mathrm{TE}, \mathrm{TM}$), respectively, below and above the discontinuity plane D. Moreover, one has

$$\begin{cases} \langle \Phi_i^{(k)}, f_{mi}^{(\alpha)} \rangle = 2\int_0^{a/2} \Phi_i^{(k)}(x) f_{mi}^{(\alpha)^*}(x)dx \\ \langle \Psi_i^{(k)}, f_{mi}^{(\alpha)} \rangle = 2\int_0^{a/2} \Psi_i^{(k)}(x) f_{mi}^{(\alpha)^*}(x)dx, \\ \quad \text{for } i = \{x, z\} \text{ and } \alpha = \mathrm{TE}, \mathrm{TM}. \end{cases} \tag{22}$$

The analytical expression of modes $f_m^{(\alpha)}$ is given in (23) at the bottom of the page, with

$$\sigma_m = \begin{cases} 1, & \text{for } m = 0 \\ 2, & \text{for } m \neq 0. \end{cases}$$

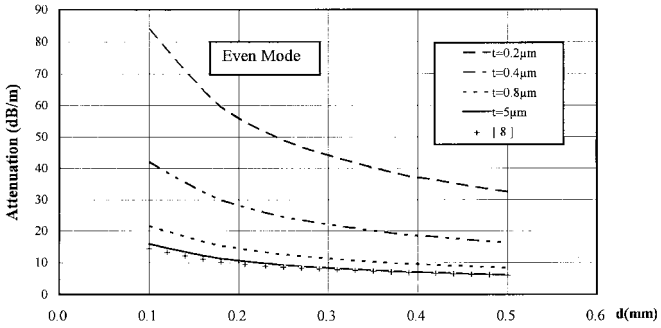

Fig. 6. Effect of metallization thickness t on the attenuation constant for a CPW even mode. Comparison with the Mirshekar *et al.* model applied to thick metals (+++++++) [8]: $a = 3.556$ mm, $b_1 = 3.4925$ mm, $h = 0.127$ mm, $b_2 = 3.4925$ mm, $w = 0.1$ mm, $\varepsilon_r = 2.22$, frequency is 27 GHz and $\sigma = 3.3\ 10^7(\Omega\mathrm{m})^{-1}$.

$$\begin{array}{lll} & p = 2k-1 & p = 2k \\ & \langle g_p, \hat{H}_{11} g_q \rangle = \sum_{\substack{m \\ \alpha=\mathrm{TE},\mathrm{TM}}} \langle \Phi_x^{(k)}, f_{mx}^{(\alpha)} \rangle H_{11m}^{(\alpha)} \langle f_{mx}^{(\alpha)}, \Phi_x^{(k')} \rangle & \langle g_p, \hat{H}_{11} g_1 \rangle = \sum_{\substack{m \\ \alpha=\mathrm{TE},\mathrm{TM}}} \langle \Phi_z^{(k)}, f_{mz}^{(\alpha)} \rangle H_{11m}^{(\alpha)} \langle f_{mx}^{(\alpha)}, \Phi_x^{(k')} \rangle \\ & \langle g_p, \hat{H}_{12} h_q \rangle = \sum_{\substack{m \\ \alpha=\mathrm{TE},\mathrm{TM}}} \langle \Phi_x^{(k)}, f_{mx}^{(\alpha)} \rangle H_{12m}^{(\alpha)} \langle f_{mx}^{(\alpha)}, \Psi_x^{(k')} \rangle & \langle g_p, \hat{H}_{12} h_q \rangle = \sum_{\substack{m \\ \alpha=\mathrm{TE},\mathrm{TM}}} \langle \Phi_z^{(k)}, f_{mz}^{(\alpha)} \rangle H_{12m}^{(\alpha)} \langle f_{mx}^{(\alpha)}, \Psi_x^{(k')} \rangle \\ q = 2k'-1 & \langle h_p, \hat{H}_{21} g_q \rangle = \sum_{\substack{m \\ \alpha=\mathrm{TE},\mathrm{TM}}} \langle \Psi_x^{(k)}, f_{mx}^{(\alpha)} \rangle H_{21m}^{(\alpha)} \langle f_{mx}^{(\alpha)}, \Phi_x^{(k')} \rangle & \langle h_p, \hat{H}_{21} g_q \rangle = \sum_{\substack{m \\ \alpha=\mathrm{TE},\mathrm{TM}}} \langle \Psi_z^{(k)}, f_{mz}^{(\alpha)} \rangle H_{21m}^{(\alpha)} \langle f_{mx}^{(\alpha)}, \Phi_x^{(k')} \rangle \\ & \langle h_p, \hat{H}_{22} h_q \rangle = \sum_{\substack{m \\ \alpha=\mathrm{TE},\mathrm{TM}}} \langle \Psi_x^{(k)}, f_{mx}^{(\alpha)} \rangle H_{22m}^{(\alpha)} \langle f_{mx}^{(\alpha)}, \Psi_x^{(k')} \rangle & \langle h_p, \hat{H}_{22} h_q \rangle = \sum_{\substack{m \\ \alpha=\mathrm{TE},\mathrm{TM}}} \langle \Psi_z^{(k)}, f_{mz}^{(\alpha)} \rangle H_{22m}^{(\alpha)} \langle f_{mx}^{(\alpha)}, \Psi_x^{(k')} \rangle \\ & \langle g_p, \hat{H}_{11} g_q \rangle = \sum_{\substack{m \\ \alpha=\mathrm{TE},\mathrm{TM}}} \langle \Phi_x^{(k)}, f_{mx}^{(\alpha)} \rangle H_{11m}^{(\alpha)} \langle f_{mz}^{(\alpha)}, \Phi_z^{(k')} \rangle & \langle g_p, \hat{H}_{11} g_q \rangle = \sum_{\substack{m \\ \alpha=\mathrm{TE},\mathrm{TM}}} \langle \Phi_z^{(k)}, f_{mz}^{(\alpha)} \rangle H_{11m}^{(\alpha)} \langle f_{mz}^{(\alpha)}, \Phi_z^{(k')} \rangle \\ & \langle g_p, \hat{H}_{12} h_q \rangle = \sum_{\substack{m \\ \alpha=\mathrm{TE},\mathrm{TM}}} \langle \Phi_x^{(k)}, f_{mx}^{(\alpha)} \rangle H_{12m}^{(\alpha)} \langle f_{mz}^{(\alpha)}, \Psi_z^{(k')} \rangle & \langle g_p, \hat{H}_{12} h_q \rangle = \sum_{\substack{m \\ \alpha=\mathrm{TE},\mathrm{TM}}} \langle \Phi_z^{(k)}, f_{mz}^{(\alpha)} \rangle H_{12m}^{(\alpha)} \langle f_{mz}^{(\alpha)}, \Psi_z^{(k')} \rangle \\ q = 2k' & \langle h_p, \hat{H}_{21} g_q \rangle = \sum_{\substack{m \\ \alpha=\mathrm{TE},\mathrm{TM}}} \langle \Psi_x^{(k)}, f_{mx}^{(\alpha)} \rangle H_{21m}^{(\alpha)} \langle f_{mz}^{(\alpha)}, \Phi_z^{(k')} \rangle & \langle h_p, \hat{H}_{21} g_q \rangle = \sum_{\substack{m \\ \alpha=\mathrm{TE},\mathrm{TM}}} \langle \Psi_z^{(k)}, f_{mz}^{(\alpha)} \rangle H_{21m}^{(\alpha)} \langle f_{mz}^{(\alpha)}, \Phi_z^{(k')} \rangle \\ & \langle h_p, \hat{H}_{22} h_q \rangle = \sum_{\substack{m \\ \alpha=\mathrm{TE},\mathrm{TM}}} \langle \Psi_x^{(k)}, f_{mx}^{(\alpha)} \rangle H_{22m}^{(\alpha)} \langle f_{mz}^{(\alpha)}, \Psi_z^{(k')} \rangle & \langle h_p, \hat{H}_{22} h_q \rangle = \sum_{\substack{m \\ \alpha=\mathrm{TE},\mathrm{TM}}} \langle \Psi_z^{(k)}, f_{mz}^{(\alpha)} \rangle H_{22m}^{(\alpha)} \langle f_{mz}^{(\alpha)}, \Psi_z^{(k')} \rangle \end{array} \tag{20}$$

$$\begin{array}{lll} & \alpha = \mathrm{TE}_x & \alpha = \mathrm{TM}_x \\ f_{mx}^{(\alpha)} & \sqrt{\frac{\sigma_m}{a}} \frac{j\beta}{\sqrt{|\beta|^2+\left(\frac{m\pi}{a}\right)^2}} \cos\left(\frac{m\pi x}{a}\right) e^{-j\beta\cdot z}, & \sqrt{\frac{\sigma_m}{a}} \frac{(m\pi/a)}{\sqrt{|\beta|^2+\left(\frac{m\pi}{a}\right)^2}} \cos\left(\frac{m\pi x}{a}\right) e^{-j\beta\cdot z} \\ f_{mz}^{(\alpha)} & \sqrt{\frac{\sigma_m}{a}} \frac{-(m\pi/a)}{\sqrt{|\beta|^2+\left(\frac{m\pi}{a}\right)^2}} \sin\left(\frac{m\pi x}{a}\right) e^{-j\beta\cdot z}, & \sqrt{\frac{\sigma_m}{a}} \frac{-j\beta}{\sqrt{|\beta|^2+\left(\frac{m\pi}{a}\right)^2}} \sin\left(\frac{m\pi x}{a}\right) e^{-j\beta\cdot z} \end{array} \tag{23}$$

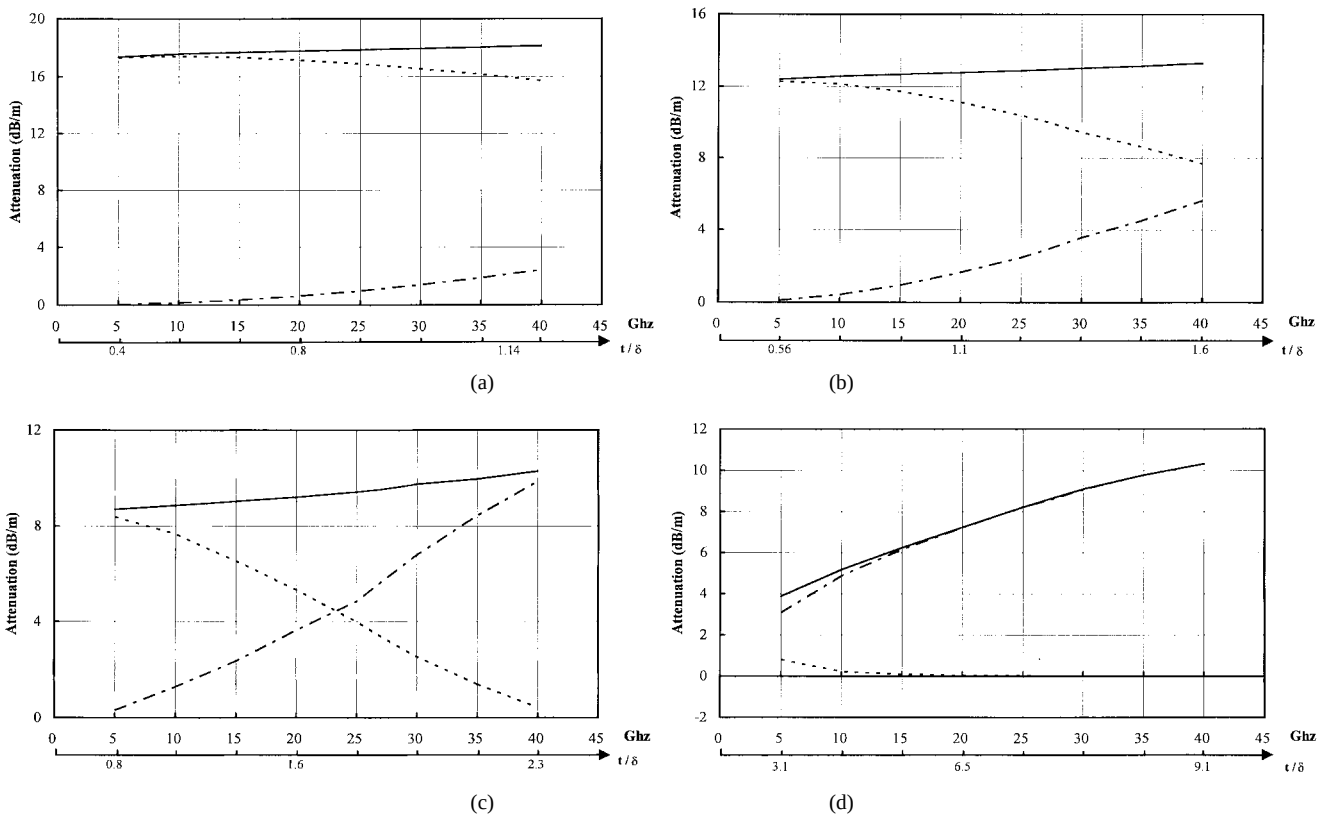

Fig. 7. Results versus frequency f and metallization thickness t. 1) The usual surface impedance models—thin conducting strips model: $Z_{s_{\text{thin}}} = 1/\sigma t$ (----------), thick conducting strips model: $Z_{s_{\text{thick}}} = Z_\sigma \coth\gamma_\sigma t$ (·-·-·-·-·), 2) The two-port model : (_____) with: (a) $t = 0.5$ μm, (b) $t = 0.7$ μm, (c) $t = 1$ μm, and (d) $t = 4$ μm and $w = 0.1$ mm, $d = 0.3$ mm, $a = 3.556$ mm, $b_1 = 3.4925$ mm, $h = 0.127$ mm, $b_2 = 3.4925$ mm, $\varepsilon_r = 2.22$ and $\sigma = 3.3\ 10^7$ $(\Omega\text{m})^{-1}$.

In the context of the above-mentioned perturbational method, the wavenumber β appearing in (23) is real; consequently, the set of $f_m^{(\alpha)}$ constitutes an orthonormal basis.

III. Numerical Results

In Fig. 6, the normalized constant attenuation of the CPW for even mode as a function of metallization thickness t and aperture width d is shown. Preliminary computations showing that $P = Q = 10$ and giving a (10×10) matrix size is sufficient for deriving accurate results of a normalized attenuation constant. The results obtained by [8], based on the perturbation technique combined with the spectral-domain method, are reported for a comparison. As shown, the metallic losses are inversely proportional to metallization thickness t and aperture width d. As the metallization thickness increases, the losses decrease. The high attenuation constant for thin conductors ($t = 0.2$ μm or $t = 0.375\delta$) decrease to remain constant for thick conductors ($t \geq 5$ μm or $t \geq 9.38\delta$). The perturbation technique results [8] agree well with this paper's numerical results when $t \geq 5$ μm, proving its validity for thick conductors.

In Fig. 7, the attenuation constant obtained by the authors' formulation is compared, which is based on the two-port model with the results obtained by usual surface impedance models [see (5) and (6)]. The normalized attenuation constant is calculated as a function of the frequency with metallization thickness ranging between 0.5 μm and 4 μm. For the metallization thickness $t = 0.5$ μm [on Fig. 7(a)] the thin conductor model results (5) agrees well with the authors' normalized attenuation below to 20 GHz (i.e., for $t \leq \delta$). Increasing the frequency up to 40 GHz, where t becomes $t = 1.14\delta$, thin conductor model results (5) represent 87% of total metallic losses, but the thick conductor model (6) provides about 11%. It is concluded that for a metallization thickness $t = 0.5$ μm with a frequency less or equal to 20 GHz, the usual thin conductor model correctly describes the metallic losses, contrary to thick conductor model (6). Fig. 7(d) demonstrates the results for a metallization thickness $t = 4$ μm, that is to say $t = 3.23\delta$ at 5 GHz and $t = 9.13\delta$ at 40 GHz. It is thus observed that the major part of losses can be obtained by the thick model. However, in the case of intermediate metallization thickness [see Fig. 7(b) and 7(c)] where $t = 0.7$ μm and 1 μm or $0.56\delta < t < 1\delta$ at 5–40-GHz frequency range, the authors remark that none of the usual surface impedance models [see (5) and (6)] can correctly characterize the metallic losses. The behavior of these two models, which varies according to the frequency, shows their limits for intermediate metallization thickness ($t \approx \delta$). This handicap is surmounted by the authors' approach (the two-port model).

In Fig. 8, the authors summarize the previous results for 27 GHz, showing the normalized attenuation constant as a function of normalized metallization thickness (t/δ). Also, the behavior of the usual surface impedance models and the two-

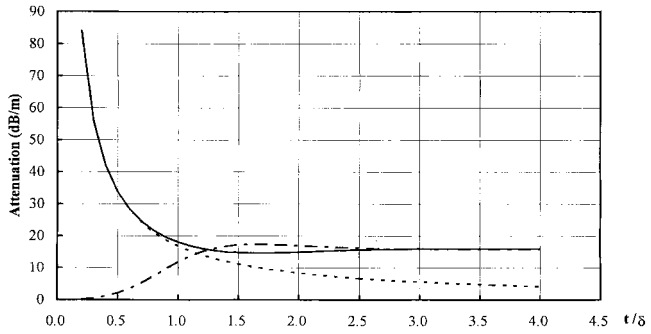

Fig. 8. Normalized metallization thickness t/δ dependence of attenuation constant α.Comparison of the two-port model with usual surface impedance models. 1) Thin conducting strips model: $Z_{s_{\text{thin}}} = 1/\sigma t$ (----------), 2) thick conducting strips model: $Z_{s_{\text{thick}}} = Z_\sigma \coth\gamma_\sigma t$ (·-·-·-·-·), 3) two-port model: (——) with $a = 3.556$ mm, $b_1 = 3.4925$ mm, $h = 0.127$ mm, $b_2 = 3.4925$ mm, $w = 0.1$ mm, $d = 0.1$ mm, $\varepsilon_r = 2.22$, frequency: 27 GHz and $\sigma = 3.3\ 10^7\ (\Omega\cdot\text{m})^{-1}$.

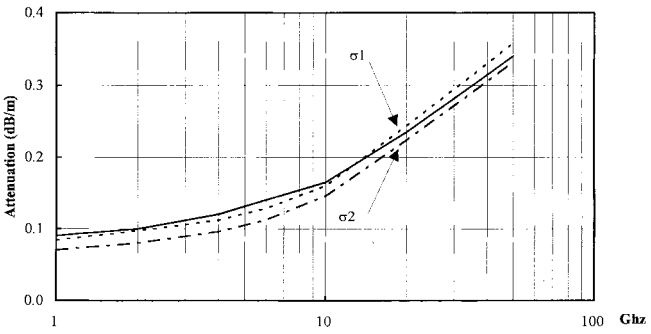

Fig. 9. Attenuation constant in a CPW with $\sigma_1 = 3.3\ 10^7\ (\Omega\cdot\text{m})^{-1}$: (----------), $\sigma_2 = 4.1\ 10^7\ (\Omega\cdot\text{m})^{-1}$: (·-·-·-·-·); experimental data [5] with $\sigma = 4.1\ 10^7\ (\Omega\text{m})^{-1}$: (——) and $a = 200\ \mu$m, $b_1 = 200\ \mu$m, $h = 200\ \mu$m, $b_2 = 0$ mm, $w = 37.5\ \mu$m, $w + 2d = 50\ \mu$m, $\varepsilon_r = 12.9$ and $t = 2.8\ \mu$m.

port model are reported. In the same manner as before, the validity of the thin conductor model (5) for $t < 1\delta$ and the thick model (6) for $t > 2\delta$ is observed. However, one can clearly see that none of these usual models can characterize the losses for intermediate metallization thickness.

Fig. 9 shows the frequency dependence of the attenuation constant for a CPW transmission line with a perfect background plane. A comparison between the authors' numerical results and measurements [5] is plotted. Due to the skin effect, the attenuation constant increases for higher frequencies. Measured values with gold finite conductivity ($\sigma = 4.1\ 10^7(\Omega\cdot\text{m})^{-1}$) are slightly less than numerical ones; however, the measured conductivity is usually smaller than the real value owing to inhomogeneous material and the roughness surface effect [4]. Therefore, one has to compute the attenuation constant for the new value of $\sigma = 3.3\,10^7(\Omega\cdot\text{m})^{-1}$. Consequently, numerical and measured results agree well, thus confirming the validity of the authors' approach.

IV. Conclusion

Equivalent network representation involving two generalized trial quantities enables the easy derivation of integral equations for a lossy CPW. The introduction of a particular two-port model for lossy conductors in this network allows one to take into account the thickness of metallization. Thus, the attenuation constant is determined without restricting the study to a single surface impedance approximation. The obtained numerical results are in very good agreement with experimental data available in the literature and with results given by the mode-matching technique. The size of matrix involved in the authors' formulation is only twice as large as the lossless case. Therefore, the effectiveness of the proposed approach based on the equivalent network representation of boundary and continuity conditions involving generalized trial quantities [16] is demonstrated in this paper. The authors' formulation can be easily applied to multilayered transmission lines including superconducting metallization.

References

[1] S. T. Peng, C. K. C. Tzuang, and C. D. Chen, "Full-wave analysis of lossy transmission line incorporating the metal modes," in *1990 IEEE MTT-S Dig.*, Session D3, pp. 171–174, 1990.

[2] W. K. Wang and C. K. C. Tzuang, "Full-wave analyzes of composite-metal multidielectric lossy microstrips," *IEEE Microwave Guided Wave Lett.*, vol. 1, pp. 97–99, May 1991.

[3] C. K. C. Tzuang, C. D. Chen, and S. T. Peng, "Full-wave analysis of lossy quasi-planar transmission line incorporating the metal modes," *IEEE Trans. Microwave Theory Tech.*, vol. 38, pp. 1792–1799, Dec. 1990.

[4] W. Heinrich, "Full-wave analysis of conductor losses on MMIC transmission lines," *IEEE Trans. Microwave Theory Tech.*, vol. 38, pp. 1468–1472, Oct. 1990.

[5] K. Beilenkoff, W. Heinrich, and H. L. Hartnagel, "Modeling of transmission line structures in coplanar MMIC's," in *Conf. Proc. MIOP'93*, Messehalle Sindelfingen, Germany, May 25–27, 1993, pp. 35–36.

[6] T. Rozzi, F. Moglie, A. Morini, E. Marionna, and M. Politi, "Hybrid modes, substrate leakage, and losses of slotline at millimeter-wave frequencies," *IEEE Trans. Microwave Theory Tech.*, vol. 38, pp. 1069–1078, Aug. 1990.

[7] N. K. Das and D. M. Pozar, "Full-wave spectral-domain computation of material, radiation and guided wave losses in infinite multilayered printed transmission lines," *IEEE Trans. Microwave Theory Tech.*, vol. 39, pp. 54–63, Jan. 1991.

[8] D. Mirshekar-Syahkal and J. B. Davies, "An accurate, unified solution to various fin-line structures, of phase constant, characteristic impedance and attenuation," *IEEE Trans. Microwave Theory Tech.*, vol. MTT-30, pp. 1854–1861, Nov. 1982.

[9] C. M. Krowne, "Microstrip conductor losses calculated by full-wave and perturbational approaches," *Electron. Lett.*, vol. 24, no. 9, pp. 552–553, Apr. 1988.

[10] J. C. Liou and K. M. Lau, "Analysis of slow-wave transmission lines on multilayered semiconductor structures including conductor losses," *IEEE Trans. Microwave Theory Tech.*, vol. 41, pp. 824–829, May 1993.

[11] H. J. Finlay, R. H. Jansen, J. A. Jenkins, and I. G. Eddison, "Accurate characterization and modeling of transmission lines for GaAs MMIC'S," *IEEE Trans. Microwave Theory Tech.*, vol. 36, pp. 961–967, June 1988.

[12] T. E. Van Deventer, P. B. Katehi, and A. C. Cangellaris, "An integral equation method for the evaluation of conductor and dielectric losses in high-frequency interconnects," *IEEE Trans. Microwave Theory Tech.*, vol. 37, pp. 1964–1972, Dec. 1989.

[13] H. Y. Lee and T. Itoh, "Phenomenological loss equivalence method for planar quasi-TEM transmission lines with a thin normal conductor or superconductor," *IEEE Trans. Microwave Theory Tech.*, vol. 37, pp. 1904–1909, Dec. 1989.

[14] L. Lewin, "A method of avoiding the edge current divergence in pertubation loss calculations," *IEEE Trans. Microwave Theory Tech.*, vol. MTT-32, pp. 717–719, July 1984.

[15] R. W. Jackson, "Considerations of the use of coplanar waveguide for millimeter-wave integrated circuits," *IEEE Trans. Microwave Theory Tech.*, vol. MTT-34, pp. 1450–1456, Dec. 1986.

[16] H. Baudrand, H. Aubert, D. Bajon, and F. Bouzidi, "Equivalent network representation of boundary conditions involving generalized trial quantities, Part I: Theory," *Annal. Télécommun.*, to be published.

[17] V. Gobin, J. P. Aparicio, J. Grando, and J. C. Alliot, "The surface impedance: A pertinent parameter to describe finite conductivity mate-

rials in numerical codes," in *9th Int. Zürich Symp. and Tech. Exhibition on Electromagnetic Compatability*, Mar. 1991, pp. 469–473.
[18] S. Ramo, J. Whinnery, and T. V. Duzer, *Field and Waves in Communication Electronics*. New York: Wiley, 1965, p. 301.
[19] D. Nghiem, J. T. Williams, and D. R. Jackson, "A general analysis of propagation along multiple-layer superconducting stripline and microstrip transmission lines," *IEEE Trans. Microwave Theory Tech.*, vol. 39, pp. 1553–1565, Sept. 1991.
[20] J. M. Ponds, C. M. Krowne, and W. C. Carter, "On the application of complex resistive boundary conditions to model transmission lines consisting of very thin superconductors," *IEEE Trans. Microwave Theory Tech.*, vol. 37, pp. 181–189, Jan. 1989.
[21] F. Bouzidi, H. Aubert, D. Bajon, H. Baudrand, and V. F. Hanna, "Equivalent circuit representation of lossy coplanar waveguides," *Annal. Telecommun.*, vol. 47, nos. 11–12, pp. 551–554, Nov.–Dec. 1992.
[22] H. Aubert, B. Souny, and H. Baudrand, "Origin and avoidance of spurious solutions in transverse resonance method," *IEEE Trans. Microwave Theory Tech.*, vol. 41, pp. 450–456, Mar. 1993.

Farid Bouzidi was born in Biskra, Algeria, in 1966. He received the Dipl.-Ing. degree from the University of Setif, Algeria, the DEA degree from the National Polytechnic Institute, Toulouse, France, and the Ph.D. degree from the Aeronautic and Space National School, "SupAero" in Toulouse, France, all in electronics engineering, in 1989, 1990, and 1994, respectively.

His research interest is numerical modeling of microwave and millimeter-wave structures, especially transitions and metallic losses in coplanar waveguides.

Hervé Aubert (M'94) was born in Toulouse, France, in 1966. He received the Dipl.-Ing. degree and the Ph.D. degree (with honors), both in electrical engineering, from the National Polytechnic Institute, Toulouse, France, in 1989 and 1993, respectively.

From January 1993 to August 1994, he was an Assistant Research Scientist at the Electrical Engineering and Signal Processing Laboratory of ENSEEIHT, Toulouse, France, and Teaching Assistant at the National Polytechnic Institute. Since September 1994, he has been an Assistant Professor of microwaves in the Department of Electrical Engineering at ENSEEIHT. His research interest is in the modeling of passive microwave and millimeter-wave integrated circuits by integral equations formulation and by variational approaches. Currently, his research activities involve the study of spurious modes in numerical methods, the equivalent network representation of boundary conditions, the discontinuity problems in waveguiding structures, and the calculation of metallic losses in printed circuits.

Dr. Aubert is a member of the New York Academy of Sciences. In 1994, he has been awarded the Leopold Escande Prize for his Ph.D. dissertation.

Damienne Bajon (M'92) was born in Toulouse France. She received the M.Sc. degree from the University Paul Sabatier, Toulouse, France, and the Ph.D. degree in electrical engineering from National Institute Polytechnic, Toulouse, France, in 1981 and 1985, respectively.

She had been on the research staff at the Laboratoire de Microondes of ENSEEIHT, Toulouse, France, and then joined the Electronics Department of the Aeronautic and Space National School, ENSAE "SupAero," 31055 Toulouse, France, as an Assistant Professor in 1989. Her research interest are in computational electromagnetics applied to modeling of microwave active components, millimeter-wave passive components, and planar structures. Her current interest is the study of numerical methods for optimizing computational efficiency of integral methods.

Henri Baudrand (M'86–SM'90) was born in France in 1939. He received the Diplome d'Ingénieur degree in electronics and the Docteur-és-Science degree in microwaves, both from the National Institute Polytechnic, Toulouse, France, in 1962 and 1966, respectively.

Since 1966, he has been working on the modeling of active and passive microwave circuits by integral methods in the Laboratoire de Microondes, ENSEEIHT, Toulouse, France. Currently, he is a Professor of microwaves and is in charge of the Microwaves Research Group. He has published approximately 80 papers.

Dr. Baudrand is Doctor Honoris Causa of University Iasi, and Chairman of the French chapter of IEEE-Microwave Theory and Techniques and the IEEE Electron Devices Societies.